

Article

# Population Structure, Genetic Diversity, and Gene Introgression of Two Closely Related Walnuts (*Juglans regia* and *J. sigillata*) in Southwestern China Revealed by EST-SSR Markers

Xiao-Ying Yuan, Yi-Wei Sun, Xu-Rong Bai, Meng Dang, Xiao-Jia Feng, Saman Zulfiqar and Peng Zhao \* 

Key Laboratory of Resource Biology and Biotechnology in Western China, Ministry of Education, College of Life Sciences, Northwest University, Xi'an 710069, China; xiaoyingy0601@163.com (X.-Y.Y.); 18634629755@163.com (Y.-W.S.); 15891710893@sina.com (X.-R.B.); 15339260798@163.com (M.D.); gongzy1993@126.com (X.-J.F.); samanch5@gmail.com (S.Z.)

\* Correspondence: pengzhao@nwu.edu.cn; Tel./Fax: +86-29-88302411

Received: 20 September 2018; Accepted: 12 October 2018; Published: 16 October 2018



**Abstract:** The common walnut (*Juglans regia* L.) and iron walnut (*J. sigillata* Dode) are well-known economically important species cultivated for their edible nuts, high-quality wood, and medicinal properties and display a sympatric distribution in southwestern China. However, detailed research on the genetic diversity and introgression of these two closely related walnut species, especially in southwestern China, are lacking. In this study, we analyzed a total of 506 individuals from 28 populations of *J. regia* and *J. sigillata* using 25 EST-SSR markers to determine if their gene introgression was related to sympatric distribution. In addition, we compared the genetic diversity estimates between them. Our results indicated that all *J. regia* populations possess slightly higher genetic diversity than *J. sigillata* populations. The Geostatistical IDW technique ( $H_O$ ,  $PPL$ ,  $N_A$  and  $PrA$ ) revealed that northern Yunnan and Guizhou provinces had high genetic diversity for *J. regia* while the northwestern Yunnan province had high genetic diversity for *J. sigillata*. AMOVA analysis revealed that significant genetic variation was mainly distributed within population as 73% in *J. regia* and 76% in *J. sigillata*. The genetic differentiation ( $F_{ST}$ ) was 0.307 between the two walnut species ( $p < 0.0001$ ), which was higher than  $F_{ST}$  values within populations (*J. regia*  $F_{ST} = 0.265$  and *J. sigillata*  $F_{ST} = 0.236$ ). However, the STRUCTURE analysis of the *J. regia* and *J. sigillata* populations revealed two genetic clusters in which gene introgression exists, therefore, the boundary of separation between these two walnut species is not clear. Moreover, these results were validated by NJ and UPGMA analysis with additional conformation from the  $PCoA$ . Based on the SSR data, our results indicate that *J. sigillata* is an ecotype of *J. regia*. Taken together, these results reveal novel information on population genetics and provide specific geographical regions containing high genetic diversity of the *Juglans* species sampled, which will assist in future conservation management.

**Keywords:** genetic diversity; genetic structure; iron walnut; common walnut; EST-SSR; introgression; southwestern China; *Juglans regia*; *Juglans sigillata*

## 1. Introduction

Walnuts trees have been valued since ancient times for their edible nuts and high-quality timber [1,2]. Walnuts belong to the family Juglandaceae (genus *Juglans*) which includes more than 20 species, with the most well-known being *J. regia* L. (common walnut) [1–5]. The *Juglans* have a diploid genome with a

karyotype of  $2n = 2x = 32$  [3]. All *Juglans* are monoecious, wind-pollinated, and temperate deciduous trees [1,4,5].

China is the third largest in-shell walnut producer, with a production of 1,700,000 tons annually [6,7]. The iron walnut (*J. sigillata* Dode) is a thick-shelled, edible walnut that grows in southwestern China and is closely related to the widely cultivated *J. regia* [8–11]. *J. sigillata* is one of the most desirable and economically valuable hardwood timber tree species found in southwestern China. Moreover, this species holds great religious and cultural importance in the region [11,12]. Both *J. regia* and *J. sigillata* have been cultivated in China for thousands of years. Therefore, China is a major center for studying walnut genetic diversity and serves as a source for germplasm used in walnut breeding [13]. In southwestern China, *J. regia* and *J. sigillata* display sympatric distribution, most notably in the Yunnan and Guizhou provinces, but also in Tibet [9,11]. Such distributions should enable the detection and extent of gene introgression between the two species and within different populations.

Whether *J. regia* and *J. sigillata* are legitimately distinct taxa in China has been controversial, but what is clear is that they freely hybridize and represent closely related gene pools. There is evidence of introgression between the two species in regions of sympatry, barring incomplete lineage sorting [4]. Previous studies of *J. regia* and *J. sigillata* mostly involved morphology, quality selection, and detecting the genetic structure of populations in different geographic regions [9,11]. Aradhya et al. [14] used ITS, RFLP, and cpDNA sequence data to suggest *J. regia* and *J. sigillata* are distinct species [14]. Moreover, Grimshaw [15] considered *J. sigillata* a distinct species based on morphology. However, a study by Wang et al. [16] on the genetic diversity and structure of nine walnut populations (five of *J. regia* and four of *J. sigillata*) in central and southwestern China (Yunnan province) found that genetic variation between populations was only about 19%, supporting the opposing view that *J. regia* and *J. sigillata* are the same species [8]. Wild *J. regia* and *J. sigillata* populations from Sichuan province have been studied using AFLPs to understand the genetic relationships between these two economically important species in the province [17,18]. In accordance with these results, Gunn et al. [11] determined that *J. regia* and *J. sigillata* are actually different ecological types of the same species based on DNA sequence data from 14 nrSSRs (simple sequence repeats) [11]. Their genetic differentiation might be a consequence of geographic migration and reproductive isolation, however, this still needs to be evaluated [11]. Wang et al. [9] analyzed a total of 209 walnut trees from nine populations (five *J. regia* and four *J. sigillata*) in Tibet using 12 nrSSRs and suggested that introgression between *J. regia* and *J. sigillata* may explain their close relationship [16]. However, little is known about the genetic diversity, structure, gene introgression and landscape genetics of *J. regia* and *J. sigillata* populations, especially in regions of sympatric distribution in southwestern China.

Closely related species can be an important source of genetic diversity for crop improvement, however, diversity estimates for many related tree crops are lacking. The majority of studies involving *J. regia* and *J. sigillata* in China have focused on their genetic diversity, cultivar development, and nutritional value [9,13,19]. However, the data are still limited and do not fully reveal introgression among them. Thus, in the present study, we analyzed population genetics, structure, and introgression of *J. regia* and *J. sigillata* from southwestern China using 25 EST-SSR (expressed sequence tag-simple sequence repeat) markers from 28 populations. Our sampled sites included Guizhou, Sichuan, and Yunnan provinces, where *J. regia* and *J. sigillata* have a sympatric distribution. Our main objectives were to (1) examine whether introgression has occurred among sympatric *J. regia* and *J. sigillata* and the likelihood of gene flow among them; (2) evaluate the genetic relationships among the populations of the two species; and (3) characterize intraspecific genetic diversity within these closely related species using EST-SSRs.

## 2. Materials and Methods

### 2.1. Sampling and DNA Extraction

Leaf samples from a total of 506 individuals from 28 populations of *J. regia* and *J. sigillata* were collected within the main range of their sympatric distribution in Yunnan, Guizhou, and Sichuan province of southwestern China (15 populations from *J. regia* ( $n = 190$ ) and 13 populations from *J. sigillata* ( $n = 316$ ), details in Table S1). Most leaf samples were collected from primary forests in rural locations. On average, the distance between collections for each population was greater than 500 m while the distance of individuals between a pair of populations within the same species was greater than 200 meters. Samples of *J. regia* and *J. sigillata* were identified based on their morphology including leaflet number (5–9 in *J. regia* and 9–11 in *J. sigillata*), flower, nut, and shell (*J. regia* has a wrinkled fruit surface; *J. sigillata* has deep pits and seal-like depressions) [20]. Fresh leaves were first dried with silica gel prior to high-quality genomic DNA extraction using a modified CTAB method [21,22] and storage at  $-20\text{ }^{\circ}\text{C}$  at the Evolutionary Botany Lab, Northwest University, Xi'an, China. DNA samples deriving from *J. regia* are designated by an “r” suffix and *J. sigillata* by an “s” suffix.

### 2.2. PCR Amplification and SSR Genotyping

All 506 individuals were genotyped using 25 loci of simple sequence repeats of expressed sequence-tagged sites (EST-SSRs) [23–26] (detailed see Table 1). All PCR amplification was carried out on an Applied Biosystems® Veriti® 96-Well Thermal Cycler (Thermo Fisher Scientific, Waltham, MA, USA) with the following method: 5 min at  $94\text{ }^{\circ}\text{C}$ , followed by 30 cycles of 45 s at  $94\text{ }^{\circ}\text{C}$ , 30 s at the specific annealing temperature ( $T_m$ ) for each marker, 90 s at  $72\text{ }^{\circ}\text{C}$  and a final extension of 5 min at  $72\text{ }^{\circ}\text{C}$ . The total volume of each PCR reaction was 20  $\mu\text{L}$  which included 2  $\mu\text{L}$  of template DNA (10 ng/ $\mu\text{L}$ ), 2.8  $\mu\text{L}$  of ddH<sub>2</sub>O, 2.0  $\mu\text{L}$  of bovine serum albumin (100 mg/L), 10  $\mu\text{L}$  2 × Taq PCR Master Mix (0.1 U Taq polymerase/ $\mu\text{L}$ ; 500  $\mu\text{M}$  each dNTP; 20 mM Tris-HCl pH 8.3; 100 mM KCl; 3.0 mM MgCl<sub>2</sub>, Tiangen, Beijing, China), and 0.4  $\mu\text{M}$  of each primer (Shagon Biotech, Shanghai, China) [26]. Upper primers were labeled with different fluorescence: FAM, HEX, TAMRA, and ROX (Sangon, Shanghai, China). Polymorphisms were checked by 10% polyacrylamide gels, with DNA bands visualized by silver nitrate staining. The amplified EST-SSRs were then purified and sequenced by Sangon (Sangon Biotech, Shanghai, China). All 506 samples were genotyped using the ABI 3730XL sequencing system (Applied Biosystems, Foster City, CA, USA) and analyzed with GeneMarker® HID (SoftGenetics, LLC., State College, PA, USA [27]).

### 2.3. Genetic Diversity Analysis

Genetic diversity per locus and between populations was evaluated through the following descriptive summary statistics: number of alleles ( $N_A$ ), observed ( $H_O$ ) and expected ( $H_E$ ) heterozygosity, Percentage of polymorphic loci ( $PPL$ ), Private alleles ( $PrA$ ), Shannon index ( $I$ ), and Fixation Index ( $F$ ) using the program GenAlEx6.5 [28]. The presence of null alleles was monitored using MICRO-CHECKER 2.2.3 [29]. Arlequin 3.5 [30] was used to test the Hardy-Weinberg equilibrium (HWE), to calculate  $F_{ST}$  for identification of potential outlier loci under selection, and for determination of Analysis of molecular variance (AMOVA) for investigation into genetic variations among and within populations for each species and species pair using 10,000 permutations. Prior to AMOVA analysis, populations TC-r, DL-r, HD-r, and WXT-r were removed due to low sample size (3–6 individuals per population). The linkage disequilibrium (LD) for all loci was tested using FSTAT [31]. GenAlEx6.5 was used to conduct a Mantel test [32] and analyze the correlation between geographical distance and genetic distance.

### 2.4. Genetic Structure Analysis

An analysis to detect genetic structure was performed using STRUCTURE (Pritchard Lab, Stanford University, Stanford, CA, USA, version 2.3.4) with a burn-in of 200,000 Markov Chain Monte Carlo

(MCMC) iterations, a duration of 500,000 iterations, ten replicates per run for  $K$  (from 2 to 10 clusters), and the admixture model [33,34]. STRUCTURE was run based on 15 neutral loci, 10 selected loci, and all 25 EST-SSR loci (Figures S1 and S2) using four datasets: (1) all samples from *J. regia* and *J. sigillata* (Table S1), (2) seven pairs of the main populations displaying sympatric distribution of *J. regia* and *J. sigillata*, (3) all fifteen populations of *J. regia*, and (4) all thirteen populations of *J. sigillata*. The program STRUCTURE HARVESTER was used to calculate the optimal value of  $K$  using the deltaK criterion [35]. The inferred clusters were drawn as colored box-plots using the program DISTRUCT [36]. Principal coordinate analysis (PCoA) was performed with GenAlEx 6.5 [28]. In order to detect signatures of bottlenecks in studied populations, the program Bottleneck 1.2 was used [37] and excess heterozygosity in each population was assessed by applying the two-tailed Wilcoxon's sign-rank test [38].  $P$  values associated with bottleneck tests were calculated by performing 10,000 permutations under both the two-phase model (TPM) and stepwise mutation model (SMM).

### 2.5. Genetic Barrier Analysis

The presence of genetic barriers, employed to highlight geographical features corresponding to pronounced genetic discontinuity, was investigated using Monmonier's maximum difference algorithm as implemented in BARRIER 2.2 [39].

### 2.6. Landscape Genetics

The Inverse Distance Weighted (IDW) [8,40] interpolation function implemented in the Geographic Information System (GIS) software ArcGIS 9.3 (ESRI, Redlands, CA, USA) was used to display the geographic patterns of observed heterozygosity ( $H_O$ ), percentage of polymorphic loci (PPL), the number of alleles ( $N_A$ ), and private alleles ( $PrA$ ) of the 28 populations sampled and to derive maps of genetic diversity. The IDW algorithm used a linear weighted combination of a set of sample points to estimate the value of a target variable in a new position. IDW assumed that points close to each other are more relevant than those that are more distant and is weighted more closely to the predicted position than the farther distances [40].

### 2.7. Inter-Specific Gene Flow

MIGRATE 3.6.4 [41] was used to estimate the historical gene flow parameter ( $M$ ) and the frequency of migration events through coalescent history between *J. regia* and *J. sigillata* for the EST-SSRs. The mode and 95% highest posterior density were then estimated after checking for data convergence.

### 2.8. Phylogenetic Relationship Analysis

The genetic relationship among populations was explored by generating neighbor-joining (NJ) trees [42] and the unweighted pair-group method with arithmetic means (UPGMA) tree using the software POPTREE2 [43] based on Nei genetic distance [44] and visualized with the software Fig Tree 1.4.2 [45].

**Table 1.** Characterization of 25 microsatellite (EST-SSRs) loci from *Juglans* populations in China.

Locus	Repeats	Primer Sequence (5′–3′)	Products	T <sub>m</sub> (°C)	N <sub>A</sub>	F <sub>IS</sub>	F <sub>IT</sub>	F <sub>ST</sub>	P <sub>HW</sub>	Nm	Reference
	Motif(s)		Range (bp)								
JC8125	(TCT)7	F: AGCAACCAGAGCAGAGCATT R: AACCTCAACACCAACTATGCT	256–268	55	1.964	0.361	0.633	0.426	***	0.337	[23]
JM5969	(AG)10	F: ACAATAGTCTCTGCACCGCC R: AGCTTGACTTACCGCCGAC	205–233	55	6.036	−0.016	0.194	0.206	ND	0.962	[26]
JH89978	(GGT)6	F: ACCTTCCCTGCTCCTCTCTT R: GAGCCTTGTTGGAAGCAAACG	183–189	55	1.464	−0.004	0.392	0.395	ND	0.383	[25]
JC7329	(TGA)8	F: TGCAGCGCATCAGTGAGTTA R: ACGCTCGAGTGTAGTAGCAAG	368–380	55	1.143	0.153	0.362	0.247	***	0.761	[23]
JM61666	(GA)11	F: AACTGTTGCCGGAGCTTTCT R: TGGGATAACACCACATGCAGT	269–271	55	1.036	−0.018	0.991	0.991	***	0.002	[26]
JR4964	(GGGA)5	F: CTCGATCTGAACTCGGCTCC R: TCTACTCTCTCCGACCACA	289–213	55	1.929	0.071	0.633	0.604	***	0.164	[24]
JR4616	(AGAC)5	F: AGCCCTTTTGCATCGGCTAT R: AGCTGACCGATCGATCAACA	160–172	55	2.286	−0.321	0.002	0.245	ND	0.772	[24]
JC5411	(GAT)7	F: AAGCTGTTTGTGCCAAAAGC R: TTCTAGCGAGAATTCCGGCC	256–262	55	1.036	−0.481	−0.012	0.317	ND	0.538	[23]
JC2995	(GA)10	F: AACTGTTGCCGGAGCTTTCT R: TGGGATAACACCACATGCAGT	268–270	58	1.000	0.000	1.000	1.000	***	0.000	[23]
JH42753	(GCT)6	F: CAGTTTTGGCCAGCTGCAAT R: TGTGCCCATGCTAAGACTGG	165–177	55	2.571	−0.180	0.196	0.318	***	0.535	[25]
JH86514	(TTAGGG)6	F: CGTTACGTCGGGAGGATGAG R: CCTCGTTCGTAGTCTCAGCC	133–151	55	2.286	−0.176	0.283	0.390	***	0.390	[25]
JH91908	(CTG)7	F: GAAAAGCATGGTCCTGCTGC R: ATTGAGCGACGAAAAGGGGT	176–206	55	3.071	−0.090	0.335	0.390	***	0.392	[25]
JR3773	(CTGT)5	F: GGTGGTTTGACCCTTAATTCTGT R: ACCCTGCCACAATGACCAAA	162–178	55	2.786	0.009	0.221	0.214	***	0.920	[24]

Table 1. Cont.

Locus	Repeats Motif(s)	Primer Sequence (5′–3′)	Products Range (bp)	T <sub>m</sub> (°C)	N <sub>A</sub>	F <sub>IS</sub>	F <sub>IT</sub>	F <sub>ST</sub>	P <sub>HW</sub>	Nm	Reference
JR1165	(AGAT) <sub>6</sub>	F: CACGTAGCGTCCGTAATCGA R: CAGCACCTCCACTAACTGCA	454–474	55	1.107	0.340	0.854	0.779	***	0.071	[24]
JH84548	(TGCA) <sub>6</sub>	F: TCTGAGGAAGCTGCATGGAA R: AACTCTGGACACATGCCGC	278–298	55	2.000	0.136	0.395	0.300	ND	0.584	[25]
JM78331	(AACGGC) <sub>5</sub>	F: GCAGTGCCTCCTTTTCAA R: TTCTCGGTTGAAGCCACAA	156–162	55	1.000	0.000	1.000	1.000	***	0.000	[26]
JR6638	(GAGG) <sub>6</sub>	F: TGGAACCGGCATCAGAAACA R: CACAGTTGATTGAGTTGCCAGT	246–162	55	0.750	0.319	0.906	0.862	***	0.040	[24]
JM68820	(ACAT) <sub>14</sub>	F: TCCTTCTGTGTGAGTGCGTG R: GGTCAGGTGAGTGGAGCAAA	220–256	55	2.571	0.305	0.678	0.536	***	0.216	[26]
JR6439	(TGCG) <sub>5</sub>	F: TCGATGCGATCATCTCCGTG R: CGGCACAAAACAGAACTCG	146–162	55	2.714	−0.090	0.266	0.327	NS	0.515	[24]
JR3434	(GTAT) <sub>5</sub>	F: CCGCCAGCAGATTGTCATA R: CGTCCCCCAAGTCTTGCT	276–296	58	1.786	−0.004	0.529	0.531	***	0.221	[24]
JH6044	(CCA) <sub>7</sub>	F: CCTCGTCTCCTCCCCTAACA R: GTAGGATAGTGTGGCGTCCG	208–270	60	2.214	0.030	0.463	0.447	***	0.310	[25]
JR6160	(GA) <sub>10</sub>	F: ACTTCAGGTTCCCAACGCAA R: TAGAGGGAAGGTCTCCGGTG	179–201	58	4.286	−0.011	0.224	0.233	***	0.824	[24]
JR1817	(AC) <sub>11</sub>	F: CCTCAGAGCCAACCATCCTT R: AGAACAGAACCAGCGTCACA	201–303	58	4.321	0.387	0.553	0.271	***	0.672	[24]
JR3147	(CTAT) <sub>6</sub>	F: CAGCACCTCCACTAACTGCA R: CACGTAGCGTCCGTAATCGA	454–478	55	1.250	0.376	0.861	0.777	NS	0.072	[24]
JH2096	(GCA) <sub>7</sub>	F: AAGCTATGTTGGCTGCTGGT R: ATTGTTCAAGCGTTGCCCTA	258–270	55	2.000	−0.101	0.089	0.172	ND	1.201	[25]

Note: ND—Not determined; NS—Not significant; \*\*\*  $p < 0.0001$ , N<sub>A</sub>—Number of alleles, F<sub>IS</sub>—within-population inbreeding coefficient; F<sub>IT</sub>—total population inbreeding coefficient; F<sub>ST</sub>—among-population genetic differentiation coefficient; P<sub>HW</sub>—Hardy-Weinberg equilibrium; Nm—gene flow.

### 3. Results

#### 3.1. Comparisons of Genetic Diversity and Differentiation between *J. regia* and *J. sigillata*

The null allele test indicates a lower frequency of null alleles at 19 loci when compared to the threshold frequency ( $\alpha = 0.15$ ) across all the *J. regia* and *J. sigillata* populations studied while the probability of null alleles was slightly significant for the remaining six loci. No evidence was found for the presence of linkage disequilibrium (LD). The Hardy-Weinberg equilibrium (HWE) test revealed highly significant deviations for many EST-SSR loci. These deviations may result from a deficiency of heterozygosity among the *J. regia* and *J. sigillata* populations. Only two loci (JR6439 and JR3147) showed no significant deviations which suggests that almost all populations may be affected by factors of interference such as introgression, mutation, and selection by migration (Table 1).

Genetic diversity parameters for each population based on allelic frequencies are summarized in Table 2. The results indicate that all *J. regia* populations possess slightly higher genetic diversity than the *J. sigillata* populations. The mean value of alleles ( $N_A$ ) is 2.261 in *J. regia* and 2.098 in *J. sigillata*. The number of effective alleles ( $N_E$ ) per population varies from 1.053 (LM-r) and 2.139 (QZ-r) in *J. regia*, while in *J. sigillata*, the values vary between 1.269 and 1.925. For *J. regia*, the lowest observed heterozygosity ( $H_O$ ) and expected heterozygosity ( $H_E$ ) are found in Liming, Yunnan population; the highest in DL-r (0.467) and QZ-s (0.419). Both values of heterozygosity in the majority of *J. regia* populations are somewhat higher than in *J. sigillata*. Shannon's information index ( $I$ ) ranges from 0.111 to 0.735, with an average of 0.518 in *J. regia* populations, while the mean number of  $I$  is 0.449 in *J. sigillata* (Table 2). Moreover, the Percentage of Polymorphic Loci ( $PPL$ ) in *J. regia* (mean = 0.328) is higher than in *J. sigillata* (mean = 0.273), with the majority of *J. regia* populations having higher  $PPL$  values. Taken together, these values support higher genetic diversity among *J. regia* populations. The fixation index ( $F$ ) determined for most populations showed significant deviations from zero, indicating a high level of inbreeding within individuals of each population. The Wilcoxon test was used to detect possible bottlenecks in each population, and signatures of significant recent population bottlenecks were detected in LJ-r and GZ-r populations of *J. regia*, and in the TZ-s population of *J. sigillata* (Table 3).

The within-population inbreeding coefficient ( $F_{IS}$ ) varies from  $-0.481$  to  $0.387$ , with a mean of  $0.043$  (Table 1). The inbreeding coefficient determined for the total population ( $F_{IT}$ ) per locus ranges from  $-0.012$  to  $0.991$  with an average of  $0.482$ . Meanwhile, the genetic differentiation ( $F_{ST}$ ) ranges from  $0.206$  to  $0.991$ , with a mean of  $0.479$ , indicating limited gene flow and high differentiation between populations. As shown in Table 1,  $F_{IS}$  is significantly negative for many loci while significantly positive for some others.  $F_{IS}$  values that are significantly greater than zero indicate a deficiency of heterozygosity at this locus, probably as a consequence of the allelic dropout, including the presence of null alleles [46]. The AMOVA analysis revealed the percentage of variation found between *J. regia* and *J. sigillata* is  $7.311\%$  ( $p < 0.0001$ ), demonstrating that the differences between the two species is significant. Therefore, analyzing the genetic structure of the *J. regia* population and the *J. sigillata* population independently is necessary. Within the population of each species, the proportion of variance is notable based on AMOVA (*J. regia*  $73\%$ ,  $p < 0.0001$ ; *J. sigillata*  $76\%$ ,  $p < 0.0001$ ). These data indicate that higher genetic variation of *J. regia* and *J. sigillata* is mainly distributed within populations (Table 3).

**Table 2.** Genetic diversity of 28 *Juglans* populations based on 25 EST-SSR loci.

Population	Location	N	N <sub>A</sub>	N <sub>E</sub>	H <sub>O</sub>	H <sub>E</sub>	I	F	PPL	Wilcoxon Test	
										TPM	SMM
<i>Juglans regia</i>											
LM-r	Liming, Yunnan	10	1.160 ± 0.111	1.053 ± 0.090	0.124 ± 0.060	0.074 ± 0.033	0.111 ± 0.046	0.24	0.078	1.000	0.375
QZ-r	Qizong, Yunnan	22	3.080 ± 0.432	2.139 ± 0.247	0.342 ± 0.055	0.419 ± 0.050	0.735 ± 0.105	0.80	0.430	0.054	0.577
TC-r	Tacheng, Yunnan	3	1.920 ± 0.152	1.665 ± 0.129	0.353 ± 0.076	0.319 ± 0.047	0.495 ± 0.076	0.72	0.391	0.432	0.322
DL-r	Delian, Yunnan	3	2.000 ± 0.216	1.808 ± 0.195	0.467 ± 0.082	0.342 ± 0.054	0.547 ± 0.093	0.68	0.413	0.160	0.160
HD-r	Hongding, Yunnan	6	1.720 ± 0.158	1.453 ± 0.108	0.315 ± 0.079	0.230 ± 0.048	0.357 ± 0.074	0.56	0.253	0.734	0.734
SG-r	Shigu, Yunnan	11	2.520 ± 0.284	1.755 ± 0.146	0.289 ± 0.051	0.347 ± 0.047	0.593 ± 0.087	0.76	0.365	0.638	1.000
WXT-r	Weixi, Tacheng, Yunnan	6	2.080 ± 0.258	1.593 ± 0.169	0.223 ± 0.045	0.297 ± 0.053	0.501 ± 0.092	0.64	0.325	0.275	0.492
BS-r	Baoshan, Yunnan	15	1.800 ± 0.200	1.459 ± 0.163	0.245 ± 0.065	0.244 ± 0.051	0.397 ± 0.083	0.60	0.253	0.301	0.426
GY-r	Guiyang, Guizhou	11	2.440 ± 0.306	1.708 ± 0.137	0.328 ± 0.065	0.328 ± 0.049	0.555 ± 0.089	0.72	0.346	0.820	0.203
LJ-r	Lijiang, Yunnan	20	2.240 ± 0.312	1.649 ± 0.164	0.333 ± 0.069	0.298 ± 0.054	0.502 ± 0.096	0.60	0.306	<b>0.006</b>	<b>0.037</b>
YW-r	Zunyi, wujiang, Guizhou	24	2.880 ± 0.362	1.963 ± 0.163	0.355 ± 0.055	0.396 ± 0.051	0.681 ± 0.097	0.76	0.407	0.005	0.432
YN-r	Wenshan, Yunnan	14	2.400 ± 0.289	1.708 ± 0.181	0.225 ± 0.043	0.342 ± 0.052	0.582 ± 0.093	0.68	0.356	0.695	0.695
GZ-r	Guizhou	18	2.960 ± 0.402	1.872 ± 0.279	0.240 ± 0.044	0.334 ± 0.055	0.632 ± 0.111	0.76	0.344	<b>0.012</b>	<b>0.002</b>
EM-r	Emei, Sichuan	15	2.240 ± 0.273	1.653 ± 0.178	0.260 ± 0.049	0.312 ± 0.054	0.533 ± 0.092	0.68	0.326	1.000	0.570
SC-r	Nanchong, Sichuan	12	2.480 ± 0.312	1.637 ± 0.183	0.265 ± 0.055	0.307 ± 0.053	0.554 ± 0.098	0.68	0.322	1.000	0.734
mean			2.261	1.674	2.291	0.306	0.518	0.66	0.328		
<i>Juglans sigillata</i>											
LM-s	Liming, Yunnan	30	2.440 ± 0.480	1.785 ± 0.330	0.314 ± 0.062	0.313 ± 0.056	0.537 ± 0.111	0.68	0.319	0.019	0.084
QZ-s	Qizong, Yunnan	30	2.600 ± 0.490	1.875 ± 0.327	0.294 ± 0.057	0.329 ± 0.058	0.587 ± 0.116	0.72	0.334	0.110	0.380
TX-s	Tacheng, Yunnan	21	2.400 ± 0.451	1.635 ± 0.224	0.276 ± 0.061	0.298 ± 0.056	0.513 ± 0.107	0.60	0.305	0.375	0.770
DL-s	Delian, Yunnan	23	2.360 ± 0.443	1.596 ± 0.204	0.233 ± 0.052	0.289 ± 0.056	0.501 ± 0.105	0.60	0.296	0.232	0.770
HD-s	Hongding, Yunnan	20	2.080 ± 0.310	1.515 ± 0.181	0.268 ± 0.054	0.284 ± 0.052	0.470 ± 0.091	0.60	0.291	0.193	0.846
SG-s	Shigu, Yunnan	30	2.000 ± 0.294	1.408 ± 0.161	0.209 ± 0.047	0.251 ± 0.050	0.421 ± 0.087	0.60	0.256	0.301	0.734
TZ-s	Weixi, Tacheng, Yunnan	30	2.480 ± 0.497	1.925 ± 0.347	0.376 ± 0.067	0.352 ± 0.056	0.594 ± 0.113	0.68	0.359	<b>0.002</b>	<b>0.012</b>
YP-s	Yongping, Yunnan	30	1.960 ± 0.303	1.275 ± 0.131	0.253 ± 0.070	0.210 ± 0.046	0.352 ± 0.075	0.56	0.214	0.313	0.742
MD-s	Midian, Yunnan	21	1.560 ± 0.192	1.269 ± 0.136	0.285 ± 0.075	0.198 ± 0.047	0.308 ± 0.073	0.48	0.203	0.547	0.742
NH-s	Nanhua, Yunnan	27	1.960 ± 0.255	1.406 ± 0.162	0.234 ± 0.058	0.247 ± 0.051	0.411 ± 0.084	0.60	0.251	0.203	0.910
BN-s	Buna, Guizhou	22	1.960 ± 0.220	1.414 ± 0.143	0.328 ± 0.067	0.274 ± 0.047	0.439 ± 0.073	0.68	0.281	0.240	0.413
HC-s	Houchang, Guizhou	18	1.800 ± 0.258	1.368 ± 0.176	0.141 ± 0.039	0.213 ± 0.051	0.361 ± 0.088	0.56	0.220	0.301	0.652
LP-s	Liupanshui, Guizhou	14	1.680 ± 0.236	1.297 ± 0.143	0.168 ± 0.049	0.212 ± 0.047	0.342 ± 0.078	0.52	0.220	0.250	0.641
mean			2.098	1.521	0.260	0.267	0.449	0.61	0.273		

Note: N—Sample Size; N<sub>A</sub>—The number of alleles; N<sub>E</sub>—Number of Effective Alleles; PPL—Percentage of Polymorphic Loci; H<sub>O</sub>—Observed Heterozygosity, H<sub>E</sub>—Expected Heterozygosity, I—Shannon's Information Index; and F—Fixation Index; Two mutation models of microsatellites: TPM—two-phase model; SMM—stepwise mutation model. *p* values lower than 0.05 are indicated in bold.

**Table 3.** Hierarchical analyses of molecular variance (AMOVA) of *Juglans* samples based on 25 EST-SSR loci.

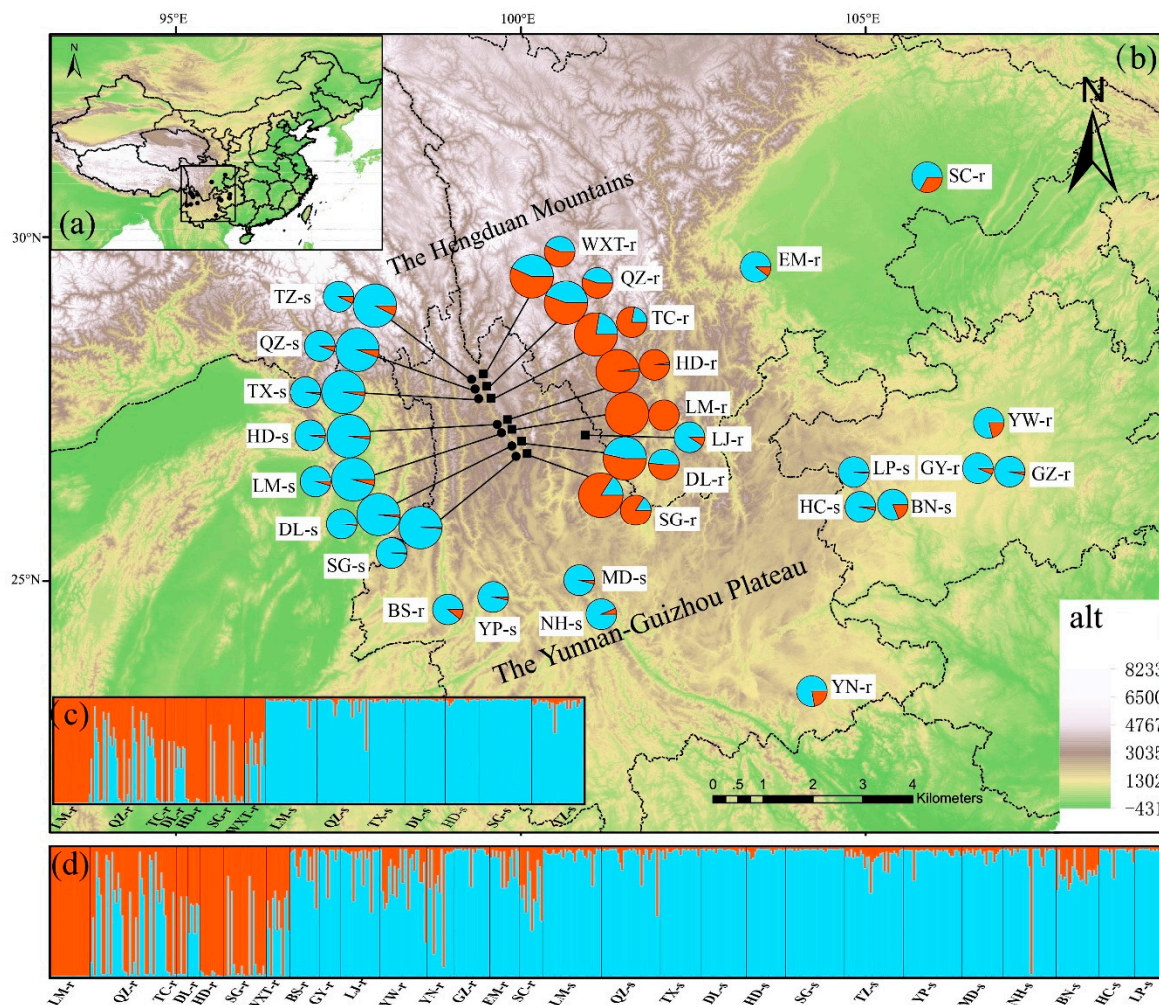
Species	Source of Variation	d.f.	SS	Variance	% Vari.	Fixation Indices
<i>JR-JS</i>	Between species	1	182.808	0.331	7.311	$F_{CT} = 0.073$ ***
	Among populations Within species	22	954.173	1.058	23.378	$F_{ST} = 0.307$ ***
	Within populations	896	2815.239	3.136	69.311	$F_{SC} = 0.252$ ***
	Total	919	3952.220	4.525		
<i>JR</i>	Among populations	10	419.903	1.352	26.482	$F_{ST} = 0.265$ ***
	Within populations	304	1148.024	3.752	73.518	
	Total	314	1567.927	5.104		
<i>JS</i>	Among populations	12	623.879	1.074	23.629	$F_{ST} = 0.236$ ***
	Within populations	569	2035.089	3.471	76.371	
	Total	581	2658.968	4.545		

*JR*—*J. regia*; *JS*—*J. sigillata*; d.f.—degrees of freedom; SS—Sum of squares; Variance—Variance components; % Vari.—Percentage of variation; 1000 permutations;  $F_{CT}$ —divergence between species;  $F_{ST}$ —divergence among populations within two species;  $F_{SC}$ —divergence among individuals within populations of two species; \*\*\*  $p < 0.001$ .

### 3.2. Spatial Genetic Structure of Populations and Divergence

The possibility exists that EST-SSRs may be located within functional genes and that the EST-SSR marker selected for study are not necessarily neutral. Inclusion of non-neutral loci may bias the population genetic diversity and genetic structure analysis. Prior to conducting genetic structure analysis, Arlequin3.5 software was used to identify possible selected loci for all 25 EST-SSRs. Ten selected loci were identified: JM5969, JM61666, JR4964, JR4616, JR3773, JR1165, JM6638, JH6160, JR3147, and JH2096 (Figure S3). Finally, 15 polymorphic and neutral EST-SSR markers were selected to assess population genetic structure among the 28 walnut populations studied herein.

The genetic structure of the 15 *J. regia* and 13 *J. sigillata* populations was inferred using STRUCTURE (Figure 1).

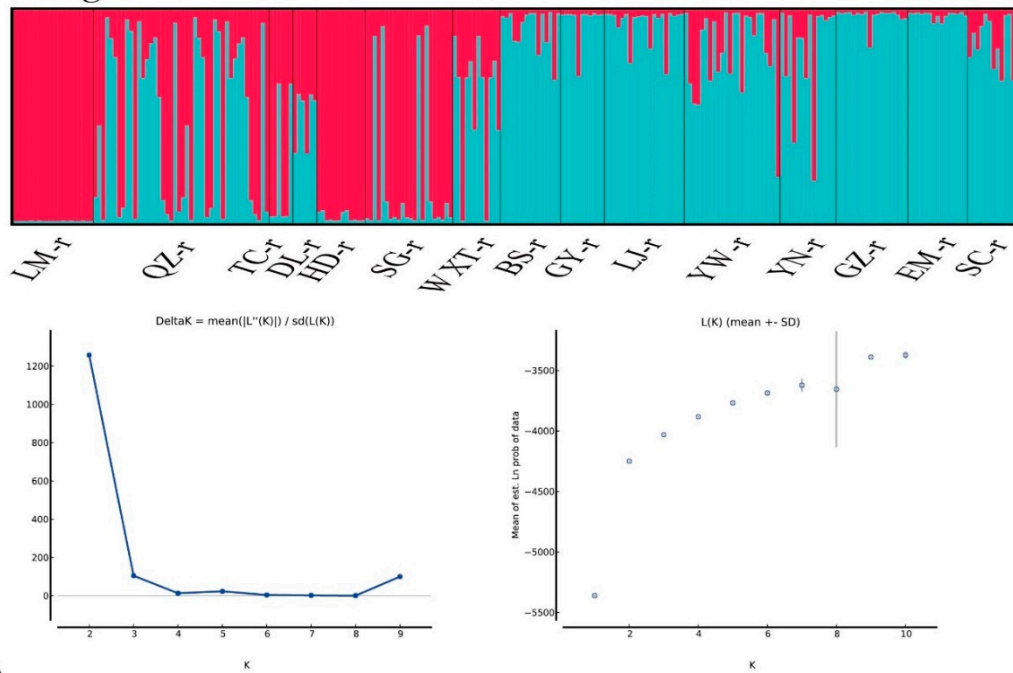
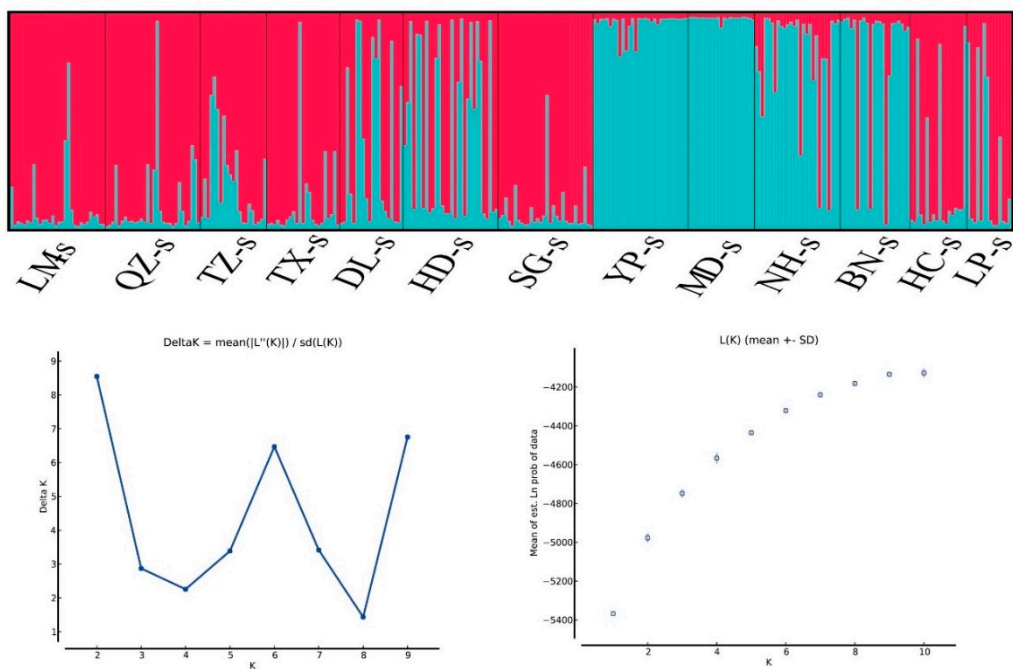


**Figure 1.** Structure clustering results for 506 individuals from 28 populations of walnut (15 *J. regia* and 13 *J. sigillata*) based on variation at 15 neutral microsatellite loci. (a) Map of China showing the region of study. (b) Geographic origin of each population sampled and their color-coded grouping ( $K = 2$  as determined using the deltaK method of Evanno et al. [34]). The location of each pie indicates the sampled locations. The larger pie chart represents the results showing the main sympatric distribution while the smaller pie chart represents the results of all populations. The proportion of colors in each pie chart reflects the proportion of genetic affiliation within each of the two populations as determined by STRUCTURE (averaged over all samples from that location). (c) Histogram of individual assignments for seven pairs of main sympatric distributions of *J. regia* and *J. sigillata*. (d) Histogram of individual assignments for all populations. Dark blue vertical lines separate the different populations as indicated by the codes below the histogram.

The optimal cluster ( $K$ ) was identified based on posterior probability ( $\Delta K$ ) values.  $K$  was tested from two to ten with 10 replicated runs performed. For seven pairs of sympatric distribution of *J. regia* and *J. sigillata*,  $\Delta K$  values computed for all classes indicated a strong signal for  $K = 2$ . This implies that the 14 sympatric populations under study are grouped into two clusters (Figure S4). Several populations displayed a clearly intermixed composition, which could be attributed to introgression among QZ-r, TC-r, DL-r, HD-r, SG-r, and WXT-r populations. When all populations were included in the STRUCTURE analysis based on EST-SSR data, the most probable division with the highest  $\Delta K$  value ( $\Delta K = 1683.81$ ) was also detected at  $K = 2$ . The results revealed two genetic clusters of *J. regia* and *J. sigillata*, which identified gene introgression among different populations; however, evidence for a distinct boundary is not apparent. Eight *J. regia* populations (BS-r, GY-r, LJ-r, YW-r, YN-r, GZ-r, EM-r, SC-r) appear to be embedded within *J. sigillata* populations based on SSRs (Figure 1). The estimated population structure inferred for  $K = 2$  is shown in Figure 1d. Results of STRUCTURE analysis using two datasets (based on only *J. regia* populations or *J. sigillata* populations) were in accordance with each other; admixture was detected between *J. regia* and *J. sigillata* and the same population genetic pattern ( $K = 2$ ) was observed (Figure 2).

Additional evidence for the genetic distribution in *J. regia* and *J. sigillata* was obtained using *PCoA* analysis (Figure 3c). The results corroborated those obtained from the STRUCTURE (Figure 1b; Figure 1c) analysis and the first three axes in Figure 3c explain 27% of the cumulative variation. The first and second coordinates accounted for nearly 15% and 22% of the molecular variation, respectively (Table S2). The individuals of *J. regia* and *J. sigillata* sampled were mostly separated by their EST-SSR data, which indicates that interspecific differentiation is stronger than intraspecific differentiation, however, considerable overlap between the *J. sigillata* and *J. regia* samples was still detected, providing additional information on the level of genomic admixture among individuals.

To further illustrate the genetic relationships among the 28 populations studied herein, a phylogenetic analysis was completed using both the Neighbor-joining (NJ) and unweighted pair-group method with arithmetic means (UPGMA) methods for tree construction, both based on Nei's genetic distances (Figure 3a,b). The resulting dendrograms revealed a high level of gene introgression between *J. regia* and *J. sigillata*, especially for several *J. regia* populations (BS-r, GY-r, LJ-r, YW-r, YN-r, GZ-r, EM-r, and SC-r) (Figure 3b). These results further support those obtained by STRUCTURE (Figure 1). At the individual level, a distinct boundary is not obvious, while introgression between these two closely related species is, however, apparent as individuals with gene introgression identified by STRUCTURE are roughly similar to *PCoA*. The resulting phylogenies are congruent and similar to the *PCoA* and STRUCTURE results, demonstrating that the *J. regia* and *J. sigillata* populations do cluster into two groups according to their presumed walnut species; however, the results also indicate gene introgression or hybridization between the different populations based on STRUCTURE analysis, NJ/UPGMA analysis, and *PCoA* analysis (Figure 1, Figure 3 and Figure S5).

**(a) *J. regia*****(b) *J. sigillata***

**Figure 2.** Structure clustering results of 15 *J. regia* and 13 *J. sigillata* populations based on variation at 15 neutral microsatellite loci. (a) The population structure based on 15 *J. regia* populations at  $K = 2$  as determined using the deltaK method of Evanno et al. [34]. (b) The population structure based on 13 *J. sigillata* populations at  $K = 2$  as determined using the deltaK method of Evanno et al. [34].

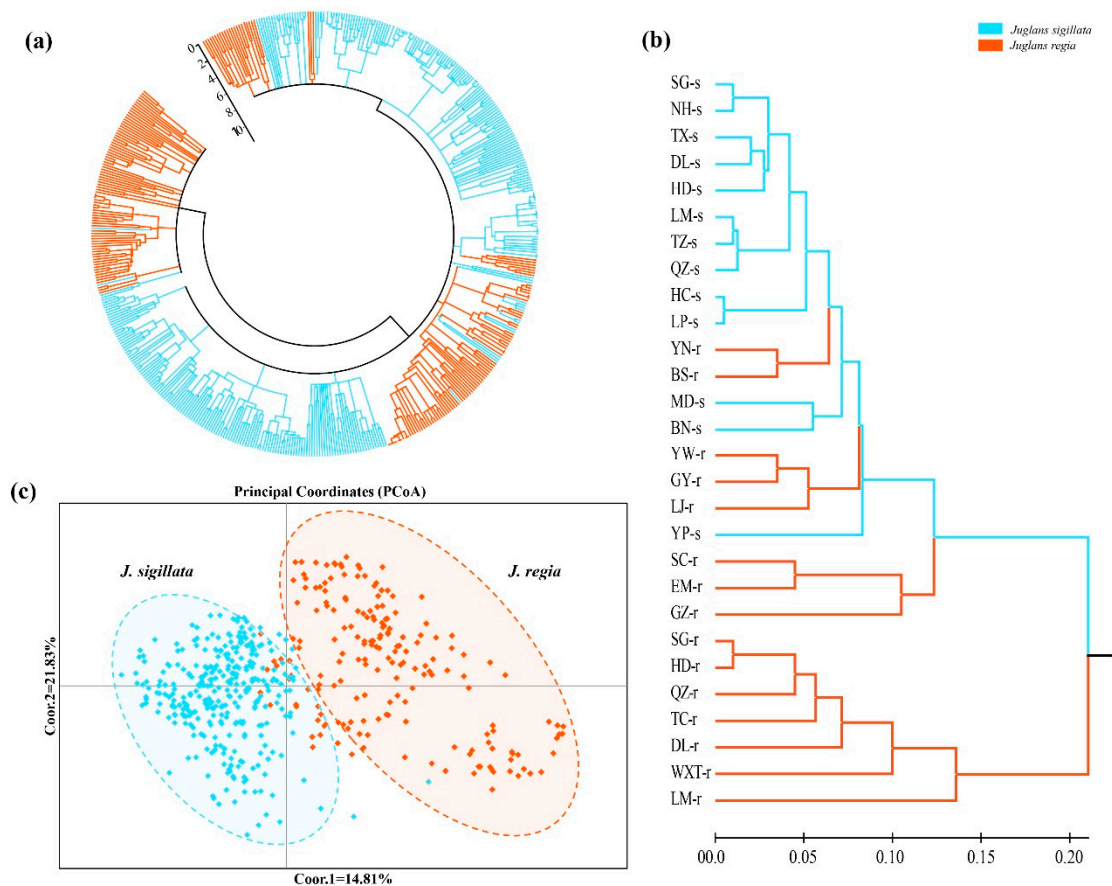


**Figure 3.** (a) Dendrogram generated by NJ cluster analysis of 506 individuals of *J. regia* and *J. sigillata* and (b) UPGMA cluster analysis of 28 *Juglans* populations (comprising of 15 *J. regia* and 13 *J. sigillata*) based on Nei's unbiased genetic distances. The letter "s" at the end of a population name indicates *J. sigillata* and "r" refers to *J. regia*. (c) Principal coordinates analysis (PCoA) of 506 individuals of *J. regia* and *J. sigillata* based on EST-SSR (25 loci). Each species is labeled with a different color, highlighting the existence of two distinct clusters.

### 3.3. Gene Introgression between *J. regia* and *J. sigillata*

The consequences of gene introgression from sympatric populations are strongly dependent on the extent of gene flow. In the Bayesian analysis of population structure, the results showed that *J. regia* individuals appear to be admixed with *J. sigillata* (Figure 1c,d). Moreover, the PCoA, NJ and UPGMA analyses confirmed the results obtained by STRUCTURE (Figure 3). The Migrate-n analysis produced  $\theta$  and  $M$  values greater than zero. The  $\theta$ -value and the size of the immigration rate ( $M$ ) revealed a highly asymmetric historical gene flow across the two species. Gene flow occurred predominantly from *J. regia* into *J. sigillata* (16.29 vs. 8.63) (Table 4, Table S4). Meanwhile, the gene flow values ( $Nm$ ) per locus ranged from 0.002 to 0.962 (average, 0.435) (Table 1). Thus, this current study provides direct evidence for historical interspecific gene flow between *J. regia* and *J. sigillata* in southwestern China.

**Table 4.** Historical gene flow as estimated by Migrate 3.6.4 among *Juglans regia* and *J. sigillata*.

Group	$\theta$	$M(m/\mu)$	
		<i>Juglans regia</i> →	<i>Juglans sigillata</i> →
<i>Juglans regia</i>	1.14[1.12–1.16]		8.63[8.09–9.19]
<i>Juglans sigillata</i>	0.66[0.64–0.67]	16.29[15.37–17.28]	

The mode of the posterior distribution is shown in bold and the values in square brackets give the 95% credibility interval;  $\theta$ ,  $4 N_e\mu$ ; →, source populations; M, mutation-scaled immigration rate; m, immigration rate;  $\mu$ , mutation rate.

### 3.4. Comparative Landscape Genetics

The genetic diversity of *J. regia* and *J. sigillata* were investigated by a landscape genetic overlay approach in southwestern China which offers promise for evaluating the important role of landscape in shaping the genetic diversity of the two species. The values of observed heterozygosity ( $H_O$ ), percentage of polymorphic Loci ( $PPL$ ), the number of alleles ( $N_A$ ) (reported in Table 2), and private alleles ( $PrA$ ) (summarized in Table S3), are geographically displayed in Figure 4. The geospatial interpolation of these indices allowed the generation of new spatial data representing the genetic diversity of *J. regia* and *J. sigillata* populations in southwestern China. The observed heterozygosity ( $H_O$ ) values of *J. regia* ranged between 0.124 (LM-r) and 0.467 (DL-r) (Table 2). High values of  $H_O$  were observed in *J. regia* populations located in the north of its distribution in Yunnan and Guizhou provinces, while lower values of  $H_O$  were shown in Sichuan and in the western and southern regions in the Yunnan populations (Figure 4a). In *J. sigillata*, significant differences among populations were observed for the values of observed heterozygosity ( $H_O$ ) (Figure 4b) where higher numbers of  $H_O$  were observed in the Himalayas (which decreased to the west) and some populations from Yunnan province, while lower values were observed in the other regions including some populations from Sichuan and Guizhou provinces. In addition, for *J. regia*, higher values of Percentage of Polymorphic Loci ( $PPL$ ) and the number of alleles ( $N_A$ ) were observed in most of the populations from Guizhou and Sichuan provinces while some of the populations from northwestern Yunnan province had the lowest numbers (Figure 4c,e). Meanwhile, in *J. sigillata*, the highest values of Percentage of Polymorphic Loci ( $PPL$ ) and the number of alleles ( $N_A$ ) are found in the area of the northwestern Yunnan (Himalayas), while regions of low  $PPL$  values were found in some populations from Yunnan and Guizhou provinces (Figure 4d,f). High values for private alleles were detected in most of Guizhou province (*J. regia*) and Yunnan province (*J. sigillata*) (Figure 4g,h). Taken together, these results reveal regions with high levels of genetic diversity that could be the result of gene flow and be associated with genetic drift. Local populations with a high genetic diversity of private alleles may be more primitive. In fact, the results of Monmonier's maximum difference algorithm implemented in BARRIER identified three statistically significant ( $0.10 < p < 0.40$ ) genetic barriers in *J. regia* and *J. sigillata* (Figures S6 and S7) in accordance with the hot map of genetic diversity. The main genetic boundary was mainly distributed in the area of Guizhou province (*J. regia*) and Yunnan (*J. sigillata*) province.

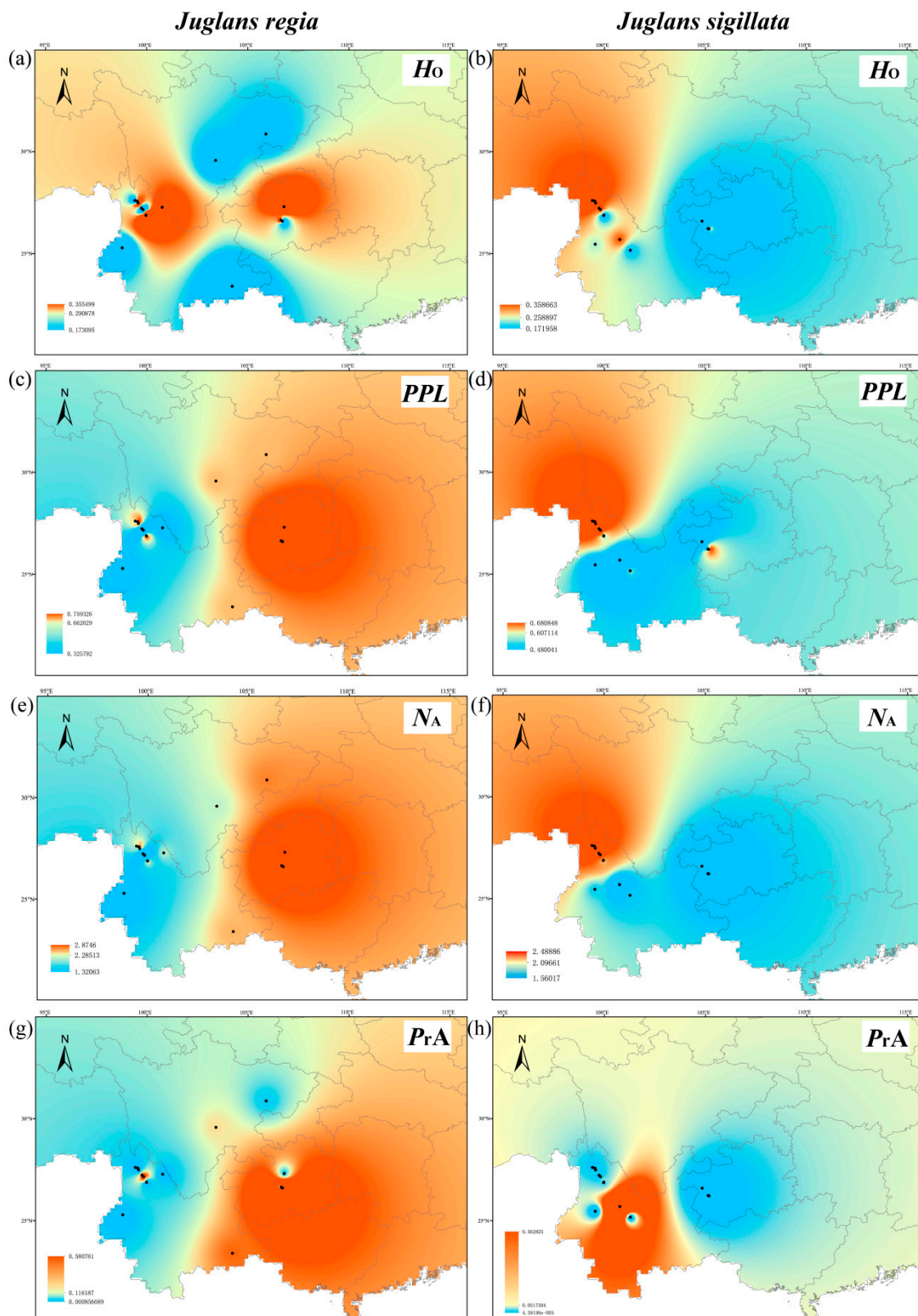


**Figure 4.** Genetic diversity maps of 15 *Juglans regia* and 13 *J. sigillata* populations (black dots) in China: IDW interpolation of (a) observed heterozygosity ( $H_0$ ) values of *J. regia*, (b) observed heterozygosity ( $H_0$ ) values of *J. sigillata*, (c) Percentage of Polymorphic Loci (PPL) values of *J. regia*, (d) Percentage of Polymorphic Loci (PPL) values of *J. sigillata*, (e) the Number of Alleles ( $N_A$ ) values of *J. regia*, (f) the Number of Alleles ( $N_A$ ) values of *J. sigillata*, (g) Private alleles ( $PrA$ ) values of *J. regia*, and (h) Private alleles ( $PrA$ ) values of *J. sigillata*.

## 4. Discussion

### 4.1. Relationship of Two Closely Related Walnut Species

*J. regia* and *J. sigillata* have been previously considered ecotypes of the same species [8–11]. In southern China, human dispersal brought *J. regia* into contact with *J. sigillata*, which is now maintained as a landrace [47]. The geographic distribution of *J. sigillata* is restricted to Yunnan and Guizhou provinces, while *J. regia* occurs in Yunnan province, Guizhou province, and Tibet [11]. The typical phenotypic differences found between *J. sigillata* and *J. regia* are considered distinct, including morphology of the flower, nut, and shell [20]. The genetic differentiation ( $F_{ST}$ ) between *J. regia* and *J. sigillata* is 0.307 ( $p < 0.0001$ ), which is slightly higher than the  $F_{ST}$  values among populations of both *J. regia* ( $F_{ST} = 0.265$ ) or *J. sigillata* ( $F_{ST} = 0.236$ ). Moreover, our results identified gene introgression between *J. regia* and *J. sigillata* using STRUCTURE, PCoA, and phylogenetic trees created by the Neighbor-joining (NJ) and the unweighted pair-group method with arithmetic means (UPGMA) algorithms (Table 4; Figure 1, Figure 3 and Figure S5). Taken together, *J. sigillata* was determined to be an ecotype, landrace, or sub-species of *J. regia* based on our SSR data (Figures 1 and 3). The gene introgression among *J. regia* and *J. sigillata* exists in both sympatric regions and non-sympatric regions (for example, EM-r, GZ-r, GY-r) in southwestern China (Figures 1 and 3), which indicates that these two species have no genetic barriers [9,11,16]. However, local adaptation and genetic differentiation also exists among *J. regia* and *J. sigillata* as determined by different genetic diversity parameters (Figure 4) and fueled by varying complex geographical regions in the environment (Figures 1, 2 and 4) [4,5,8].

### 4.2. Advantages of the EST-SSR Molecular Marker

There are several advantages of EST-derived SSRs over those from non-coding nuclear genomes. EST-SSRs are typically more transferrable to related species [48] and polymorphisms in EST-SSRs may be used to assess differences in gene expression, indicating adaptive differences among populations [49]. EST-SSRs typically amplify more successfully than non-genic SSRs, and EST-SSRs often have conserved primer sites, simplifying analyses [24,50]. In the particular case of *J. sigillata*, EST-SSRs are an excellent tool for studying speciation and population genetic differentiation between the closely related *J. regia*. The EST-SSRs described herein could prove useful for understanding gene flow and genetic structure in other members of the Juglandaceae as well. The population genetic structure showed that *J. regia* had a signal genetic differentiation ( $K = 4$ ) based on 10 selected EST-SSRs loci, however, *J. sigillata* showed the most probable division with the highest  $\Delta K$  value ( $\Delta K = 1683.81$ ) at  $K = 2$  and  $K = 4$  (Figure S2). In this study, the STRUCTURE results based on neutral loci and selected loci were not significantly and consistently the same in *J. regia* and *J. sigillata* (Figure 1 and Figure S1). These outcomes may be derived from adaptive evolution and local differentiation in regions of sympatric distribution in southwestern China, however, the two species did show gene introgression in this region [4,9,11].

### 4.3. Genetic Diversity, Structure, and Differentiation Patterns

Prior to this study, little was found in public databases for *J. sigillata*. Previously published studies focused on genetic diversity of a single walnut species [11,16]. Landscape genetic analysis and introgression of sympatric distribution analysis were both lacking for populations of *J. regia* and *J. sigillata* in southwestern China. In our study, we investigated the introgression of two closely related walnut species based on EST-SSR markers. Gene introgression between sympatric populations is common and can affect the genetic diversity within each species [51,52]. We found all *J. regia* populations possess slightly higher genetic diversity than the *J. sigillata* populations studied (Table 2), however, the lower genetic diversity of *J. sigillata* may be associated with our sampling range. As shown in Table 1, many loci exhibited significant deviations from Hardy-Weinberg expectations and we can detect high  $F$  values for each of the populations in both species (Table 2). These factors indicate that inbreeding was occurring between the populations in southwestern China. The level of within-population inbreeding coefficient ( $F_{IS}$ ) for each locus ranged from  $-0.481$  to  $0.387$ . Similar

results were previously found in walnut populations in Tibet and Italy [9,16,53] and in other species [54]. *J. sigillata* and *J. regia* showed a high level of genetic differentiation within their respective populations ( $F_{ST} = 0.236$ ,  $p < 0.001$  in *J. sigillata*;  $F_{ST} = 0.265$ ,  $p < 0.001$  in *J. regia*) based on EST-SSRs. The value of  $F_{ST}$  we observed was considerably larger than a previous estimate based on four populations of *J. sigillata* (11%,  $p < 0.0001$ ) and five populations of *J. regia* (10%,  $p < 0.0001$ ) [9]. One possible explanation for the relatively high  $F_{ST}$  we observed is that by using EST-SSRs, our samples captured variation caused by selection [55]. The EST-SSR loci we developed were polymorphic enough to distinguish among sympatric populations and to reveal affinities and differences. The AMOVA analysis showed a high level of genetic variation between *J. regia* and *J. sigillata*, 7 % ( $p < 0.0001$ ) (Table 3), which was considerably larger than a previous study (0.70% in Gunn et al., [11]). The Mantel test showed no significant correlation between genetic distance and geographical distance of *J. regia* ( $r = -0.065$ ,  $p = 0.27 > 0.05$ ) and *J. sigillata* ( $r = 0.05$ ,  $p = 0.32 > 0.05$ ), and the possible reason may be attributed to our small sampling range. The spatially explicit map showed that *J. regia* was fully sympatric with *J. sigillata*, and the results from STRUCTURE showed that gene introgression from *J. sigillata* to *J. regia* is significant (Figure 1). A similar division of the populations was identified by PCoA, and the division also appeared in the AMOVA, UPGMA tree and NJ tree. Furthermore, the STRUCTURE analysis showed that there are eight *J. regia* populations embedded within *J. sigillata*, likely due to human disturbance, which also may have caused the expansion of gene introgression from *J. sigillata* to *J. regia*, keeping in mind that the majority of *J. regia* was cultivated. Thus, *J. regia* may be undergoing genetic swamping by admixture with both *J. regia* and *J. sigillata*. Genetic swamping and introgression by related species can threaten genetic and evolutionary integrity of a species, which represents an important hazard to plant conservation [56]. Given that the population structure of several sympatric populations from Yunnan showed clear signs of introgression, gene flow from *J. sigillata* may have contributed to local or regional differentiation of *J. regia* populations [9,11,16]. This possibility is reinforced by the distinctiveness of *J. regia* in Yunnan province, where the distribution of both *J. regia* and *J. sigillata* naturally co-occurs [4]. The MIGRATE analysis yielded estimates of migration rates between two clusters as greater than zero, indicating that some post divergent gene flow has occurred. Furthermore, it is interesting to note that hybridization may have played a significant role in genetic differentiation, and ecologically adaptive differences could also be a contributing factor. Introgressive hybridization may increase the risk of losing autochthonous genetic diversity [57], therefore, a solid understanding of the standing genetic diversity and gene flow is vital for future species conservation.

#### 4.4. Introgression and Landscape Genetics between Sympatric Regions of *J. regia* and *J. sigillata* in Southwestern China

Previous studies could not accurately identify the relationship between *J. regia* and *J. sigillata* [9,11,14,16,19]. One possible explanation for why our results were different is that the previous research did not consider the possibility of introgression between the two species, and all of their samples were collected from regions of sympatric distributions in their studied area. Therefore, some introgression may be mistaken among the two species, leading to biased results. In particular, the consequences of introgression from sympatric populations are strongly dependent on the extent of gene flow and therefore it is essential to describe interspecific gene flow among two closely related species. Introgression could have a two-sided effect on the genetic diversity of populations. Many factors play a role in introgression including the direction of introgression and the effective population size. It was reported that in Tibet, introgression has occurred between *J. regia* and *J. sigillata*, and the direction of gene flow has been mainly from *J. regia* to *J. sigillata* [9]. The best explanation for this result is that the natural outcrossing mechanisms of the two species may determine the direction of gene flow. In our study, we found that gene introgression between *J. regia* and *J. sigillata* mainly occurred in the Yunnan area. Our identification of gene flow was based solely on EST-SSR markers between sympatric populations, which may have been caused by wind-pollination and human disturbance. Genetic barriers act as a boundary to gene flow from different populations, which may affect the

genetic differentiation of populations, leading to high genetic diversity. Genetic diversity, however, will also increase if existing gene flow between populations occurs for other reasons. In addition, landscape genetics has provided new opportunities to analyze spatial patterns of neutral or functional genetic diversity in a forest tree species [8]. It is essential to evaluate the geographical patterns of genetic diversity and identify the populations within, and determine areas that display high values of genetic diversity and divergence. However, until now, practitioners have seldom taken into account the relevance of genetics research [58] and few studies on landscape genetics have been applied in practical forest management [59]. From our point of view, landscape genetics can be considered an easy and self-explaining tool to transfer information about spatial distribution of genetic variation into practice. In this work, the application of novel spatial analysis provides more exhaustive and critical information on the genetic diversity of *J. regia* and *J. sigillata*. However, as it was discussed in a recent study, Pollegioni et al. [5] demonstrated the spatial genetic structure of walnuts in Europe using the software IDW function.

Genomic studies of introgression between closely related species are beginning to offer novel insights into the evolutionary consequences of hybridization and genetic structure. Overall, we believe that our work will provide convincing evidence for the introgression of sympatric distributions for *J. regia* and *J. sigillata* in southwestern China. Evidence for introgression between species of the genus *Juglans* is known, and its extent may be due to strong gene flow between closely related species with sympatric distributions. The polymorphic microsatellite loci and the genetic variation index used in this study are of great significance for research in the population genetics of walnut, and our findings, including locations of high genetic diversity, will play a significant role in conservation management of *J. regia* and *J. sigillata*.

## 5. Conclusions

In the current study, we analyzed population genetics, genetic structure, and introgression of *J. regia* and *J. sigillata* from southwestern China based on EST-SSR (expressed sequence tag-simple sequence repeat) markers from sympatric walnut populations. The genetic diversity of all *J. regia* populations was slightly higher than *J. sigillata* populations. STRUCTURE analysis revealed two genetic clusters of all samples, which showed gene introgression among different walnut populations, but failed to distinguish a boundary between the two species. The generation of phylogenetic trees, along with PCoA analysis, confirmed the results from STRUCTURE. Taken together, our results demonstrate that *J. sigillata* is an ecotype, landrace, or sub-species of *J. regia* based on SSR data. These combined results, with an emphasis on regions discovered with high genetic variation of each species, provide significant information on population genetics and structure of *J. regia* and *J. sigillata*, which can be used for conservation management in the future.

**Supplementary Materials:** The following are available online at <http://www.mdpi.com/1999-4907/9/10/646/s1>, Figure S1. The population structure clustering results at  $K = 2$  as determined using the deltaK method of Evanno et al. (2005). (a) Histogram of individual assignments for all 28 populations of *J. regia* and *J. sigillata* based on 25 EST-SSRs loci. (b) Histogram of individual assignments for *J. regia* and *J. sigillata* including 28 populations, based on 10 selected EST-SSRs loci. (c) Histogram of individual assignments for seven pairs of *J. regia* and *J. sigillata* populations exhibiting sympatric distribution based on 25 EST-SSR loci. (d) Histogram of individual assignments for seven pairs of *J. regia* and *J. sigillata* population exhibiting sympatric distribution based on 10 selected EST-SSRs loci. Population codes are located below the histogram. Figure S2. The population structure clustering results determined using the deltaK method of Evanno et al. (2005). (a) Histogram of individual assignments for 15 *J. regia* populations at  $K = 2$  based on 25 EST-SSRS loci. (b) Histogram of individual assignments for 15 *J. regia* populations at  $K = 4$  based on 10 selected microsatellite loci. (c) Histogram of individual assignments for 13 *J. sigillata* populations at  $K = 2$  based on 25 EST-SSRS loci. (d) Histogram of individual assignments for 13 *J. sigillata* populations at  $K = 2$  based on 10 selected microsatellite loci. Black lines separate different populations. The population codes are located below the histogram. Figure S3. Detection of loci under selection from genome scans based on  $F_{ST}$ . Figure S4. (a) Histogram of individual assignments for seven pairs of *J. regia* and *J. sigillata* populations displaying sympatric distribution for  $K = 2$ . (b,d) Distribution of delta  $K$  for  $K = 2$  to 9 to determine the true number of populations ( $K$ ) as described in Evanno et al. (2005). Mean log likelihood of the data at varying estimates of  $K$ . (c) Histogram of individual assignments for all populations for  $K = 3$ . The magnitude of  $\Delta K$  as a function of  $K$  suggests the existence of two major clusters as the most likely scenario. Figure S5. (a) Dendrogram

generated by UPGMA cluster analysis of 506 individuals of *J. regia* and *J. sigillata* and (b) NJ cluster analysis of 28 *Juglans* populations based on Nei's unbiased genetic distances. The letter of "s" at the end of population names means *J. sigillata* and "r" means *J. regia*. (c) Principal coordinates analysis (PCoA) of 28 populations from *J. regia* and *J. sigillata* based on EST-SSR (25 loci); each walnut species is labeled with two different colors, representing 506 individuals that were grouped into two clusters. Figure S6. BARRIER analyses of the main genetic barriers of *Juglans regia*. Delaunay triangulation and detected barriers with bootstrap values over 1000 replicates using Nei's genetic distances. Blue line represents del aunay triangulation, red line indicates statistically significant genetic boundaries. Figure S7. BARRIER analyses of the main genetic barriers of *Juglans sigillata*. Delaunay triangulation and detected barriers with bootstrap values over 1000 replicates using Nei's genetic distances. Blue line represents del aunay triangulation, red line indicates statistically significant genetic boundaries. Table S1. Number of samples (N), location, geographic coordinates (latitude and longitude) for 28 *Juglans* populations surveyed in southwestern China. Table S2. Percentage of variation explained by the first 3 axes using Principal Coordinate analysis for model based approach. Table S3. Description of private alleles by 12 populations. Table S4. Summary of profile likelihood percentiles of all parameters.

**Author Contributions:** Conceived and designed the experiments: P.Z.; Performed the experiments: P.Z., X.-Y.Y., Y.-W.S., X.-J.F., X.-R.B. and M.D.; Analyzed the data: P.Z., X.-J.F., X.-Y.Y., Y.-W.S., M.D., S.Z. and X.-R.B.; Contributed materials/analysis tools: P.Z.; Wrote the paper: P.Z., Y.-W.S., X.-Y.Y. and S.Z. All authors read and approved the final manuscript.

**Funding:** This research was funded by the National Natural Science Foundation of China (Grant Nos. 31200500 and 41471038), the Program for Excellent Young Academic Backbones funding by Northwest University (Grant No. 338050070), and the Northwest University Training Programs of Innovation and Entrepreneurship for Graduates (Grant Nos. 2016002, 2017037 and 2018298).

**Acknowledgments:** The authors wish to thank Xiaojia Feng, Yiwei Sun and Dang Meng for sample collection.

**Conflicts of Interest:** The authors declare no conflict of interest.

## References

- Manning, W.E. The classification within the Juglandaceae. *Ann. Mo. Bot. Gard.* **1978**, *65*, 1058–1087. [[CrossRef](#)]
- Bernard, A.; Lheureux, F.; Dirlewanger, E. Walnut: Past and future of genetic improvement. *Tree Genet. Genom.* **2018**, *14*, 1. [[CrossRef](#)]
- Woodworth, R.H. Meiosis of microsporogenesis in the Juglandaceae. *Am. J. Bot.* **1930**, *17*, 863–869. [[CrossRef](#)]
- Han, H.; Woeste, K.E.; Hu, Y.; Dang, M.; Zhang, T.; Gao, X.X.; Zhou, H.J.; Feng, X.J.; Zhao, G.F.; Zhao, P. Genetic diversity and population structure of common walnut (*Juglans regia*) in China based on EST-SSRs and the nuclear gene phenylalanine ammonia-lyase (PAL). *Tree Genet. Genom.* **2016**, *12*, 111. [[CrossRef](#)]
- Pollegioni, P.; Woeste, K.; Chiocchini, F.; Del Lungo, S.; Ciolfi, M.; Olimpieri, I.; Tortolano, V.; Clark, J.; Hemery, G.E.; Mapelli, S.; et al. Rethinking the history of common walnut (*Juglans regia* L.) in Europe: Its origins and human interactions. *PLoS ONE* **2017**, *12*, e0172541. [[CrossRef](#)] [[PubMed](#)]
- FAO (Food and Agricultural Organization of the United Nations). FAO Statistical Databases and Data Sets. 2012. Available online: <http://faostat.fao.org> (accessed on 20 September 2018).
- Golge, O.; Hepsag, F.; Kabak, B. Determination of aflatoxins in walnut sujuk and Turkish delight by HPLC-FLD method. *Food Control* **2016**, *59*, 731–736. [[CrossRef](#)]
- Pollegioni, P.; Woeste, K.E.; Chiocchini, F.; Olimpieri, I.; Tortolano, V.; Clark, J.; Hemery, G.E.; Mapelli, S.; Malvolti, M.E. Landscape genetics of Persian walnut (*Juglans regia* L.) across its Asian range. *Tree Genet. Genom.* **2014**, *10*, 1027–1043. [[CrossRef](#)]
- Wang, H.; Pan, G.; Ma, Q.; Zhang, J.; Pei, D. The genetic diversity and introgression of *Juglans regia* and *Juglans sigillata* in Tibet as revealed by SSR markers. *Tree Genet. Genom.* **2015**, *11*, 1. [[CrossRef](#)]
- Lu, A.M. On the geographical distribution of the Juglandaceae. *Acta Phytotaxon. Sin.* **1982**, *20*, 257–271.
- Gunn, B.F.; Aradhya, M.; Salick, J.M.; Miller, A.J.; Yang, Y.P.; Liu, L.; Hai, X. Genetic variation in walnuts (*Juglans regia* and *J. sigillata*; Juglandaceae): Species distinctions, human impacts, and the conservation of agrobiodiversity in Yunnan, China. *Am. J. Bot.* **2010**, *97*, 660–671. [[CrossRef](#)] [[PubMed](#)]
- Weckerle, C.; Huber, F.; Yang, Y.P.; Sun, W.B. Walnuts among the Shuhi in Shuiluo, eastern 426 Himalayas: Notes on economic plants. *Econ. Bot.* **2005**, *59*, 287–290. [[CrossRef](#)]
- Chen, L.; Ma, Q.; Chen, Y.; Wang, B.; Pei, D. Identification of major walnut cultivars grown in China based on nut phenotypes and SSR markers. *Sci. Hortic.* **2014**, *168*, 240–248. [[CrossRef](#)]

14. Aradhya, M.K.; Potter, D.; Gao, F.; Simon, C.J. Molecular phylogeny of *Juglans* (Juglandaceae), a biogeographic perspective. *Tree Genet. Genom.* **2007**, *3*, 363–378. [[CrossRef](#)]
15. Grimshaw, J. *Notes on the Temperate Species of Juglans*; International Dendrology Society: Kington, UK, 2003; pp. 107–130.
16. Wang, H.; Pei, D.; Gu, R.S.; Wang, B.Q. Genetic diversity and structure of walnut populations in central and southwestern China revealed by microsatellite markers. *J. Am. Soc. Hortic. Sci.* **2008**, *133*, 197–203.
17. Chen, L.H.; Hu, T.X.; Zhang, F.; Li, G.H. Genetic diversities of four *Juglans* populations revealed by AFLP in Sichuan province, China. *J. Plant Ecol.* **2008**, *32*, 1362–1372.
18. Chen, L.H.; Hu, T.X.; Zhang, F. AFLP analysis on genetic diversity of *Juglans* populations in dry and dry-hot valleys of Sichuan province. *J. Fruit Sci.* **2009**, *26*, 48–54.
19. Aradhya, M.K.; Potter, D.; Simon, C.J. Origin, evolution, and biogeography of *Juglans*: A phylogenetic perspective. *Int. Walnut Symp.* **2004**, *4*, 85–94. [[CrossRef](#)]
20. Xi, R.T.; Zhang, Y.P. *Fruit Trees of China*; Walnut Chinese Forestry Press: Beijing, China, 1996. (In Chinese)
21. Doyle, J.J.; Doyle, J.L. A rapid DNA isolation procedure for small quantities of fresh leaf tissue. *Phytochem. Bull.* **1987**, *19*, 11–15.
22. Zhao, P.; Woeste, K.E. DNA markers identify hybrids between butternut (*Juglans cinerea* L.) and Japanese walnut (*Juglans ailantifolia* Carr.). *Tree Genet. Genom.* **2011**, *7*, 511–533. [[CrossRef](#)]
23. Dang, M.; Liu, Z.X.; Chen, X.; Zhang, T.; Zhou, H.J.; Hu, Y.H.; Zhao, P. Identification, development, and application of 12 polymorphic EST-SSR markers for an endemic Chinese walnut (*Juglans cathayensis* L.) using next-generation sequencing technology. *Biochem. Syst. Ecol.* **2015**, *60*, 74–80. [[CrossRef](#)]
24. Dang, M.; Zhang, T.; Hu, Y.; Zhou, H.J.; Woeste, K.; Zhao, P. De novo assembly and characterization of bud, leaf and flowers transcriptome from *Juglans regia* L. for the identification and characterization of new EST-SSRs. *Forests* **2016**, *7*, 247. [[CrossRef](#)]
25. Hu, Y.H.; Zhao, P.; Zhang, Q.; Wang, Y.; Gao, X.X.; Zhang, T.; Zhou, H.J.; Dang, M.; Woeste, K.E. De novo assembly and characterization of transcriptome using Illumina sequencing and development of twenty five microsatellite markers for an endemic tree *Juglans hopeiensis* Hu in China. *Biochem. Syst. Ecol.* **2015**, *63*, 201–211. [[CrossRef](#)]
26. Hu, Z.; Zhang, T.; Gao, X.X.; Wang, Y.; Zhang, Q.; Zhou, H.J.; Zhao, G.F.; Wang, M.L.; Woeste, K.; Zhao, P. De novo assembly and characterization of the leaf, bud, and fruit transcriptome from the vulnerable tree *Juglans mandshurica* for the development of 20 new microsatellite markers using Illumina sequencing. *Mol. Genet. Genom.* **2016**, *291*, 849–862. [[CrossRef](#)] [[PubMed](#)]
27. Holland, M.M.; Parson, W. GeneMarker<sup>®</sup> HID: A reliable software tool for the analysis of forensic STR data. *J. Forensic Sci.* **2011**, *56*, 29–35. [[CrossRef](#)] [[PubMed](#)]
28. Peakall, R.; Smouse, P.E. GenAlEx 6.5: Genetic analysis in Excel. Population genetic software for teaching and research—an update. *Bioinformatics* **2012**, *28*, 2537–2539. [[CrossRef](#)] [[PubMed](#)]
29. Van Oosterhout, C.; Hutchinson, W.F.; Wills, D.P.; Shipley, P. MICRO-CHECKER: Software for identifying and correcting genotyping errors in microsatellite data. *Mol. Ecol. Resour.* **2004**, *4*, 535–538. [[CrossRef](#)]
30. Excoffier, L.; Lischer, H.E. Arlequin suite ver 3.5: A new series of programs to perform population genetics analyses under Linux and Windows. *Mol. Ecol. Resour.* **2010**, *10*, 564–567. [[CrossRef](#)] [[PubMed](#)]
31. Goudet, J. FSTAT (Version 2.9.3.): A Program to Estimate and Test Gene Diversities and Fixation Indices. Available online: [www.unil.ch/izea/software/fstat.html](http://www.unil.ch/izea/software/fstat.html) (accessed on 20 September 2018).
32. Mantel, N. The detection of disease clustering and a generalized regression approach. *Cancer Res.* **1967**, *27*, 209–220. [[PubMed](#)]
33. Pritchard, J.K.; Stephens, M.; Donnelly, P. Inference of population structure using multilocus genotype data. *Genetics* **2000**, *155*, 945–959. [[PubMed](#)]
34. Evanno, G.; Regnaut, S.; Goudet, J. Detecting the number of clusters of individuals using the software STRUCTURE: A simulation study. *Mol. Ecol.* **2005**, *14*, 2611–2620. [[CrossRef](#)] [[PubMed](#)]
35. Earl, D.A.; vonHoldt, B.M. STRUCTURE HARVESTER: A website and program for visualizing STRUCTURE output and implementing the Evanno method. *Conserv. Genet. Resour.* **2012**, *4*, 359–361. [[CrossRef](#)]
36. Rosenberg, N.A. DISTRUCT: A program for the graphical display of population structure. *Mol. Ecol. Resour.* **2004**, *4*, 137–138. [[CrossRef](#)]
37. Piry, S.; Luikart, G.; Cornuet, J. BOTTLENECK: A computer program for detecting recent reductions in the effective population size using allele frequency data. *J. Hered.* **1999**, *90*, 502–503. [[CrossRef](#)]

38. Luikart, G.; Allendorf, F.W.; Cornuet, J.M.; Sherwin, W.B. Distortion of allele frequency distributions provides a test for recent population bottlenecks. *J. Hered.* **1998**, *89*, 238–248. [[CrossRef](#)] [[PubMed](#)]
39. Manni, F.; Guerard, E.; Heyer, E. Geographic patterns of (genetic, morphologic, and linguistic) variation: How barriers can be detected by using Monmonier's algorithm. *Hum. Biol.* **2004**, *76*, 173–190. [[CrossRef](#)] [[PubMed](#)]
40. Hengl, T. *A Practical Guide to Geostatistical Mapping*; University of Amsterdam: Amsterdam, The Netherlands, 2009.
41. Beerli, P. Comparison of Bayesian and maximum-likelihood inference of population genetic parameters. *Bioinformatics* **2005**, *22*, 341–345. [[CrossRef](#)] [[PubMed](#)]
42. Saitou, N.; Nei, M. The neighbor-joining method: A new method for reconstructing the phylogenetic trees. *Mol. Biol. Evol.* **1987**, *4*, 406–425. [[PubMed](#)]
43. Takezaki, N.; Nei, M.; Tamura, K. POPTREE2: Software for constructing population trees from allele frequency data and computing other population statistics with windows interface. *Mol. Biol. Evol.* **2010**, *27*, 747–752. [[CrossRef](#)] [[PubMed](#)]
44. Nei, M. Analysis of gene diversity in subdivided populations. *Proc. Natl. Acad. Sci. USA* **1973**, *70*, 3321–3323. [[CrossRef](#)] [[PubMed](#)]
45. Rambaut, A. "FigTree, Version 1.3.1". Computer Program Distributed by the Author. Available online: <http://tree.bio.ed.ac.uk/software/figtree/> (accessed on 4 January 2011).
46. Soulsbury, C.D.; Iossa, G.; Edwards, K.J.; Baker, P.J.; Harris, S. Allelic dropout from a high-quality DNA source. *Conservat. Genet.* **2007**, *8*, 733–738. [[CrossRef](#)]
47. Zhao, P.; Zhou, H.J.; Potter, D.; Hu, Y.H.; Feng, X.J.; Dang, M.; Feng, L.; Zulfiqar, S.; Liu, W.Z.; Zhao, G.F.; et al. Population genetics, phylogenomics and hybrid speciation of *Juglans* in China determined from whole chloroplast genomes, transcriptomes, and genotyping-by-sequencing (GBS). *Mol. Phylogenet. Evol.* **2018**, *126*, 250–265. [[CrossRef](#)] [[PubMed](#)]
48. Ellis, J.R.; Burke, J.M. EST-SSRs as a resource for population genetic analyses. *Heredity* **2007**, *99*, 125–132. [[CrossRef](#)] [[PubMed](#)]
49. Bradbury, D.; Smithson, A.; Krauss, S.L. Signatures of diversifying selection at EST-SSR loci and association with climate in natural Eucalyptus populations. *Mol. Ecol.* **2013**, *22*, 5112–5129. [[CrossRef](#)] [[PubMed](#)]
50. Zhang, M.Y.; Fan, L.; Liu, Q.Z.; Song, Y.; Wei, S.W.; Zhang, S.L.; Wu, J. A novel set of EST-derived SSR markers for pear and cross-species transferability in Rosaceae. *Plant Mol. Biol. Rep.* **2014**, *32*, 290–302. [[CrossRef](#)]
51. Lexer, C.; Fay, M.F.; Joseph, J.A.; Nica, M.S.; Heinze, B. Barrier to gene flow between two ecologically divergent *Populus* species, *P. alba* (white poplar) and *P. tremula* (European aspen): The role of ecology and life history in gene introgression. *Mol. Ecol.* **2005**, *14*, 1045–1057. [[CrossRef](#)] [[PubMed](#)]
52. Shu, Z.; Zhang, X.; Yu, D.; Xue, S.; Wang, H. Natural hybridization between Persian walnut and Chinese walnut revealed by simple sequence repeat markers. *J. Am. Soc. Sci.* **2016**, *141*, 146–150.
53. Pollegioni, P.; Woeste, K.; Olimpieri, I.; Marandola, D.; Cannata, F.; Malvolti, M.E. Long-term human impacts on genetic structure of Italian walnut inferred by SSR markers. *Tree Genet. Genom.* **2011**, *7*, 707–723. [[CrossRef](#)]
54. Chen, Y.Y.; Chu, H.J.; Liu, H.; Liu, Y.L. Abundant genetic diversity of the wild rice *Zizania latifolia* in central China revealed by microsatellites. *Ann. Appl. Biol.* **2012**, *161*, 192–201. [[CrossRef](#)]
55. Narasimhamoorthy, B.; Saha, M.C.; Swaller, T.; Bouton, J.H. Genetic diversity in switchgrass collections assessed by EST-SSR markers. *Bioenerg. Res.* **2008**, *1*, 136. [[CrossRef](#)]
56. Hu, Y.; Dang, M.; Feng, X.; Woeste, K.; Zhao, P. Genetic diversity and population structure in the narrow endemic Chinese walnut *Juglans hopeiensis* Hu: Implications for conservation. *Tree Genet. Genom.* **2017**, *13*, 91. [[CrossRef](#)]
57. Fuchs, E.J.; Martínez, A.M.; Calvo, A.; Muñoz, M.; Arrieta-Espinoza, G. Genetic diversity in *Oryza glumaepatula* wild rice populations in Costa Rica and possible gene flow from *O. sativa*. *PeerJ* **2016**, *4*, e1875. [[CrossRef](#)] [[PubMed](#)]

58. Bowman, J.; Greenhorn, J.E.; Marrotte, R.R.; McKay, M.M.; Morris, K.Y.; Prentice, M.B.; Wehtje, M. On applications of landscape genetics. *Conserv. Genet.* **2016**, *17*, 753–760. [[CrossRef](#)]
59. Keller, D.; Holderegger, R.; van Strien, M.J.V.; Bolliger, J. How to make landscape genetics beneficial for conservation management? *Conserv. Genet.* **2015**, *16*, 503–512. [[CrossRef](#)]



© 2018 by the authors. Licensee MDPI, Basel, Switzerland. This article is an open access article distributed under the terms and conditions of the Creative Commons Attribution (CC BY) license (<http://creativecommons.org/licenses/by/4.0/>).